



NUMERICAL SIMULATION OF A PROPULSIVE WING

By

Eng./Hossameldin Elmoatsem Mourad

A thesis submitted to the
Faculty of Engineering at Cairo University
In Partial Fulfillment of the
Requirements for the degree of
MASTER OF SCIENCE
In
AEROSPACE ENGINEERING

NUMERICAL SIMULATION OF A PROPULSIVE WING

By

Eng./Hossameldin Elmoatsem Mourad

A Thesis Submitted to the
Faculty of Engineering at Cairo University
in Partial Fulfillment of the
Requirements for the Degree of
MASTER OF SCIENCE
in
AEROSPACE ENGINEERING

Under the Supervision of

Prof. Dr. Prof. Dr.

Mohammed Madboli Abdel-Rahman Professor of Aerodynamics Aerospace Engineering department Faculty of Engineering, Cairo University Basman Mohammed Nabil El-Hadidi Professor of Aerodynamics Aerospace Engineering department Faculty of Engineering, Some University

NUMERICAL SIMULATION OF A PROPULSIVE WING

By

Eng./Hossameldin Elmoatsem Mourad

A Thesis Submitted to the
Faculty of Engineering at Cairo University
in Partial Fulfillment of the
Requirements for the Degree of
MASTER OF SCIENCE
in
AEROSPACE ENGINEERING

Approved by the Examining Committee

Prof. Dr. Mohammed Madboli Abdel-Rahman Thesis Main Advisor

<u>Prof. Dr. Basman Mohammed Nabil El-Hadidi</u> Member

<u>Prof. Dr. Galal Bahgat Al-Shazely Salem</u> Internal Examiner

Prof. Dr. Osama Ezzat Abdellatif

External Examiner

- Professor at Mechanical Power department, Faculty of Engineering in Shubra, Banha University.

FACULTY OF ENGINEERING, CAIRO UNIVERSITY GIZA, EGYPT 2017 **Engineer's Name:** Hossameldin Elmoatasem Mourad Abdou

Date of Birth: 18/3/1982 **Nationality:** Egyptian

E-mail: eng-hossamsabar@hotmail.com

Phone: +201064822731, +201224827802, +20223450001 **Address:** 297 El-Yasmin (4), Al-tagamo' Al-Awal,

New Cairo, Cairo, Egypt.

Registration Date: 1/10/2011
Awarding Date:/2017
Degree: Master of Science
Department: Aerospace Engineering

Supervisors: Prof. Dr. Mohammed Madboli Abdel-Rahman

Prof. Dr. Basman Mohammed Nabil El-Hadidi

Examiners: Prof. Dr. Osama Ezzat Abdellatif (External examiner) (Professor

at Mechanical Power department, Faculty of Engineering in Shubra, Banha

University).

Prof. Dr. Galal Bahgat Al-Shazely Salem (Internal examiner) Prof. Dr. Mohammed Madboli Abdel-Rahman Hadidi (Thesis

main advisor)

Prof. Dr. Basman Mohammed Nabil El- Hadidi (Member)

Title of Thesis: NUMERICAL SIMULATION OF A PROPULSIVE WING **Key Words:** NUMERICAL; SIMULATION; PROPULSIVE; WING;

FANWING

Summary:

In the present thesis, Chapter 1 is an introduction to the propulsive wing and literature review of related work done in this field. In Chapter 2 the numerical model and method of calculation and the grid sensitivity analysis is presented. In Chapter 3 the results is shown. In Chapter 4 the conclusion is discussed.

The propulsive wing is examined numerically to determine the benefit and efficiency of a new proposed propulsive device. In the propulsive wing concept, the fan is embedded inside the wing section and the out flow jet blows over the wing. This pushes the aerodynamic envelope of the wing by avoiding stall up to 45° and hence maintain very high lift coefficient. The numerical model is first compared with published experimental data. The comparison shows that the K-ε model is the optimum model for the numerical calculation; a sensitivity study is then performed to determine the flight operating points of the propulsive wing based on the numerical values for the net thrust force. The numerical results show that the operating speed of the propulsive wing increases from 3.4 to 13.5 m/s as the RPM throttle setting increases from 1020 to 4200 RPM. The lift can be high as 23 N for $\alpha = 30^{\circ}$, which is not attainable with conventional wings. The airstream operating velocity (velocity required to get almost zero net thrust, is proportional to the fan speed at the same angle of attack, while it is proportional inversely with the RPM at different angles of attack; at 4200 RPM, the velocity is 21.6 m/s at $(\alpha=0^{\circ})$ while it decreases to 13.5 m/s at $(\alpha=30^{\circ})$. The relation between Lift and the fan RPM's is progressively proportioned, the lift increases with RPMs in same angle of attack, and also it increases with angles of attack for same RPM.



ACKNOWLEDGMENTS

I thank God, for helping me complete this work. During the past few years I have been on service call several times and the work seemed endless and only through patience was I able to finish.

I would like to thank Dr. Madbouli and Dr. Basman, Department of Aerospace, Faculty of Engineering, Cairo University, for their effort and time with me. The door to their office was always open whenever I ran into a trouble spot or had a question about my research or writing.

I must express my gratitude to my family and wife for providing me with unfailing support and continuous encouragement throughout my years of study and through the process of researching and writing this thesis. This accomplishment would not have been possible without them.

Thank you.

Hossameldin Elmoatasem Mourad

TABLE OF CONTENTS

Chapter	Page
ACKNOWLEDGMENTS	i
TABLE OF CONTENTS.	
LIST OF TABLES	
LIST OF FIGURES	
NOMENCLATURE	vii
ABSTRACT	viii
CHAPTER 1: INTRODUCTION AND LITERATURE REVIEW	1
1.1. History	
1.2. Literature Review	6
1.3. Objective	8
1.4. Thesis Layout	
CHAPTER 2: NUMERICAL MODEL	
2.1. Numerical Model	
2.2. Method of Calculation	
2.3. Grid Sensitivity Analysis	
CHAPTER 3: RESULTS	
3.1. Comparison of Lift and Thrust with Experimental Data	
3.2. Comparison of Flow for Different RPM's vs. Angle of Attack	
3.2.1. Angle of Attack $\alpha = 0^{\circ}$	
3.2.2. Angle of Attack $\alpha = 20^{\circ}$	
3.2.3. Angle of Attack $\alpha = 40^{\circ}$	32
3.2.4. Summary of Study	
3.3. Determination of Flight Operating Conditions	44
3.3.1. Angle of Attack $\alpha = 0^{\circ}$	45
3.3.2. Angle of Attack $\alpha = 10^{\circ}$	
3.3.3. Angle of Attack $\alpha = 15^{\circ}$	52
3.3.4. Angle of Attack $\alpha = 20^{\circ}$	55
3.3.5. Angle of Attack $\alpha = 25^{\circ}$	61
3.3.6. Angle of Attack $\alpha = 30^{\circ}$	66
CHAPTER 4: CONCLUSIONS	
REFERENCES	
Appendix A: Experimental Data	75
Appendix B: Validation Data	77

LIST OF TABLES

Table	Page
Table 1: Distributed propulsion concepts [6]	3
Table 2: FanWing and boundary Dimensions	
Table 3: FanWing mesh refinement	
Table 4: Results of FanWing mesh refinement	
Table 5: FanWing results at (0°) angle of attack	20
Table 6: FanWing results at (20°) angle of attack	26
Table 7: FanWing results at (40°) angle of attack	32
Table 8: Lift vs. AoA curves equations	
Table 9: Lift Coefficient vs. AoA curves equations	40
Table 10: Thrust vs. AoA curves equations	
Table 11: Thrust Coefficient vs. AoA curves equations	42
Table 12: FanWing iteration results at (0) angle of attack	45
Table 13: FanWing iteration results at (10°) angle of attack	49
Table 14: FanWing iteration results at (15°) angle of attack	52
Table 15: FanWing iteration results at (20°) angle of attack	55
Table 16: FanWing iteration results at (25°) angle of attack	61
Table 17: FanWing iteration results at (30°) angle of attack	66
Table 18: Operational speeds for the FanWing	70
Table 19: Lift obtained according to operational speeds	70
Table 20: Operating parameters measured using a tethered wing	76
Table 21: Comparison between Numerical and Experimental lift	77
Table 22: Comparison between Numerical and Experimental Thrust	77

LIST OF FIGURES

Figure	Page
Figure 1: Forces acting on airplane [1]	1
Figure 2: Lift generation on wing [2]	1
Figure 3: A schematic of typical airfoil [3]	2
Figure 4: Schematic of propulsive wing cross section [4]	2
Figure 5: Kinematic concept solutions [7]	4
Figure 6: Schematic wing with enclosed cross-flow fan near its leading edge	4
Figure 7: Example of Propulsive wing [8]	
Figure 8 : Cross-section trough an aircraft lifting member (wing)	5
Figure 9: FanWing model aircraft [11]	
Figure 10: Combination of FanWing and Cyclogyro aircraft [15]	
Figure 11: Schematic of FanWing	
Figure 12: Schematic of cross flow fan for FanWing	
Figure 13: Boundary Conditions	
Figure 14: Geometrical parameters of the FanWing	12
Figure 15: case (A) represents the Start case of the FanWing, case (B) represents the	
refinement of the mesh, and case (C) represents the 2 nd refinement of th	
FanWing mesh.	
Figure 16: Comparison of Thrust forces for the successive grids at different operation	
RPM's and V= 5.5 m/s and α =0°	
Figure 17: Comparison of lift forces for the successive grids at different operating	
RPM's and V= 5.5 m/s and α =0°	
Figure 18: FanWing stream function with 5.5 m/s free stream flow and (0°) angle of	
attack	
Figure 19: Contours of velocity magnitude in the FanWing	
Figure 20: Filled Contours of velocity magnitude in the FanWing	
Figure 21: Lift validation chart	
Figure 22: Thrust validation chart	
Figure 23: Stream function at (0°) angle of attack for (0) RPM fan rotation	
Figure 24: Stream function at (0°) angle of attack for (1020) RPM fan rotation	
Figure 25: Stream function at (0°) angle of attack for (2500) RPM fan rotation	
Figure 26: Stream function at (0°) angle of attack for (4200) RPM fan rotation	
Figure 27: Lift vs. Fan RPM at (0°) angle of attack and 5.5 m/s airstream velocity	
Figure 28: Thrust vs. Fan RPM at (0°) angle of attack and 5.5 m/s airstream velocity	y23
Figure 29: Gage Static pressure distribution at (0°) angle of attack for (0) RPM fan	24
rotation	24
rotation	
Figure 31: Gage Static pressure distribution at (0°) angle of attack for (2500) RPM	
rotation	
Figure 32: Gage Static pressure distribution at (0°) angle of attack for (4200) RPM	
rotation	
Figure 33: Gage Static pressure distribution on the airfoil upper and bottom walls at	
angle of attack [17]	
Figure 34: Stream function at (20°) angle of attack for (0) RPM fan rotation	

Figure 35: Stream function at (20°) angle of attack for (1020) RPM fan rotation	27
Figure 36: Stream function at (20°) angle of attack for (2500) RPM fan rotation	28
Figure 37: Stream function at (20°) angle of attack for (4200) RPM fan rotation	28
Figure 38: Lift vs. Fan RPM at (20°) angle of attack and (5.5) m/s airstream velocity	y .29
Figure 39: Thrust vs. Fan RPM at (20°) angle of attack and 5.5 m/s airstream veloci	ity 29
Figure 40: Gage Static pressure distribution at (20°) angle of attack for (0) RPM far	1
rotation	30
Figure 41: Gage Static pressure distribution at (20°) angle of attack for (1020) RPM	I fan
rotation	
Figure 42: Gage Static pressure distribution at (20°) angle of attack for (2500) RPM	I fan
rotation	
Figure 43: Gage Static pressure distribution at (20°) angle of attack for (4200) RPM	I fan
rotation	
Figure 44: Stream function at (40°) angle of attack for (0) RPM fan rotation	
Figure 45: Stream function at (40°) angle of attack for (1020) RPM fan rotation	
Figure 46: Stream function at (40°) angle of attack for (2500) RPM fan rotation	
Figure 47: Stream function at (40°) angle of attack for (4200) RPM fan rotation	
Figure 48: Lift vs. Fan RPM at 40° angle of attack and 5.5 m/s airstream velocity	
Figure 49: Thrust vs. Fan RPM at 40° angle of attack and 5.5 m/s airstream velocity	
Figure 50: Gage Static pressure distribution at (40°) angle of attack for (0) RPM far	
rotation	
Figure 51: Gage Static pressure distribution at (40°) angle of attack for (1020) RPM	
rotation	
Figure 52: Gage Static pressure distribution at (40°) angle of attack for (2500) RPM	
rotation	
Figure 53: Gage Static pressure distribution at (40°) angle of attack for (4200) RPM	
rotation	
Figure 54: Lift vs. RPM at 5.5 m/s air stream velocity	
Figure 55: Thrust vs. RPM at 5.5 m/s air stream velocity	
Figure 56: Lift vs. AoA (α) at 5.5 m/s air stream velocity	
Figure 57: Lift Coefficient (C_L) vs. AoA (α) at 5.5 m/s air stream velocity	
Figure 58: Thrust vs. AoA (α) at 5.5 m/s air stream velocity	
Figure 59: Thrust Coefficient (C_T) vs. AoA (α) at 5.5 m/s air stream velocity	
Figure 60: Lift-Thrust chart at 5.5 m/s air stream velocity	
Figure 61: Coefficient of Lift and Thrust chart at 5.5 m/s air stream velocity	
Figure 62: Determination algorithm flowchart	
Figure 63: Free stream velocity -RPM chart at (0°) angle of attack	
Figure 64: Lift-RPM chart at (0°) angle of attack	
Figure 65: Stream function at $\alpha=0^{\circ}$	
Figure 66: Free stream Velocity - Fan RPM chart at (10°) angle of attack	
Figure 67: Lift - Fan RPM chart at (10°) angle of attack	
Figure 68: Stream function at $\alpha=10^{\circ}$	
Figure 69: Free stream Velocity - Fan RPM chart at (15°) angle of attack	
Figure 70: Lift – Fan RPM chart at (15°) angle of attack	
Figure 71: Stream function at $\alpha=15^{\circ}$	
Figure 72: Free stream velocity - Fan RPM Chart at (20°) angle of attack	
Figure 73: Lift - Fan RPM Chart at (20°) angle of attack	
Figure 74: Stream function at α =20°	
Figure 75: Free stream velocity - Fan RPM Chart at (25°) angle of attack	
Figure 76: Lift - Fan RPM Chart at (25°) angle of attack	64

Figure 77: Stream function at α =25°	65
Figure 78: Free stream velocity-Fan RPM Chart at (30°) angle of attack	67
Figure 79: Lift - Fan RPM Chart at (30°) angle of attack	68
Figure 80: Stream function at α =30°	69
Figure 81: Velocity-RPM chart at different angles of attack	71
Figure 82: Lift - RPM chart at different angles of attack	71
Figure 83: Top plan view of an aircraft incorporating the lifting member of Fig. 8	75
Figure 84: Graph of fan input power plotted against lift in grams force	76

NOMENCLATURE

Symbol	Nomenclature	Unit
	Fluid density	Kg/m ³
$oldsymbol{V}$	Air stream relative velocity	m/s
P	Static pressure	N/m^2
и	x-components of velocity vector	m/s
v	y-components of velocity vector	m/s
	Shear stress	N/m ²
W	The input power of the fan measured in watts	Watt
k	The turbulence kinetic energy	N.m
V	The rate of dissipation for the turbulence kinetic energy	$J/(kg.s)=m^2/s^3$
S	Wing span	m
С	Airfoil chord	m
L	Lift force	N
T	Thrust force	N
~	viscosity	Pa.s=(N.s)/m ² =kg/(s.m)
~ _t	The turbulent (eddy) viscosity	
Vx	Air stream relative velocity in x-direction	m/s
Vy	Air stream relative velocity in y-direction	m/s
Fx	Resultant force in x-direction	N
Fy	Resultant force in y-direction	N
α	Angle of attack	Degree (°)
N	Fan rotation	RPM

ABSTRACT

In the present thesis, the propulsive wing is examined numerically to determine the benefit and efficiency of a new proposed propulsive device. In the propulsive wing concept, the fan is embedded inside the wing section and the outflow jet blows over the wing. This pushes the aerodynamic envelope of the wing by avoiding stall up to 45° and hence maintain very high lift coefficient.

The numerical model is first compared with published experimental data. The comparison shows that the K-ɛ model is the optimum model for the numerical calculation; a sensitivity study is then performed to determine the flight operating points of the propulsive wing based on the numerical values for the net thrust force.

The numerical results show that the operating speed of the propulsive wing increases from 3.4 to 13.5 m/s as the RPM throttle setting increases from 1020 to 4200 RPM. The lift can be high as 23 N for $\alpha = 30^{\circ}$, which is not attainable with conventional wings.

The airstream operating velocity (velocity required to get almost zero net thrust, is proportional to the fan speed at the same angle of attack, while it is proportional inversely with the RPM at different angles of attack; at 4200 RPM, the velocity is 21.6 m/s at $(\alpha=0^{\circ})$ while it decreases to 13.5 m/s at $(\alpha=30^{\circ})$.

The lift is found to also increase as the RPM increases at the same angle of attack. Since it is possible to delay stall, the lift increases as the angle of attack is increased as long as the RPM is sufficiently high to keep the flow attached on the upper surface.

CHAPTER 1: INTRODUCTION AND LITERATURE REVIEW

Moving an airfoil (wing) relative to the air produces aerodynamic forces of *drag* and *lift*. The *thrust force* is created by a propeller or a jet engine. There are three vectors representing the aerodynamic forces on a powered airplane: lift, drag and thrust. The other force acting on an aircraft during flight is the *weight force*.

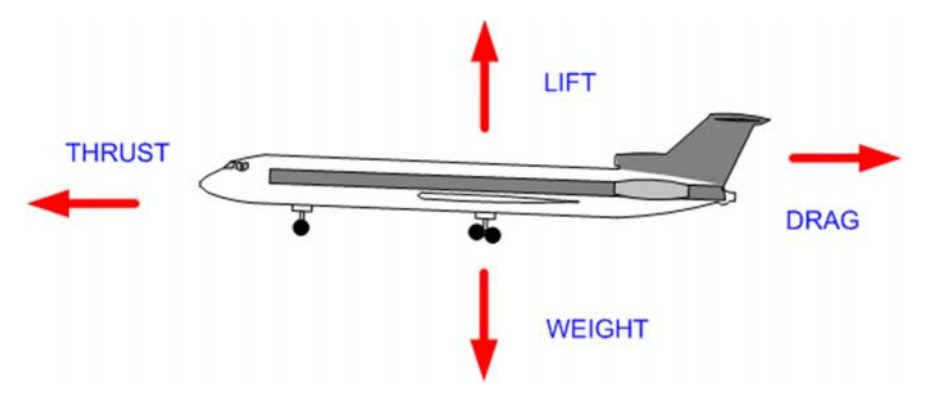


Figure 1: Forces acting on airplane [1]

In convential airfoil or wing, lift is generated by static pressure difference between upper and lower surface of the wing as shown in Fig. 2.

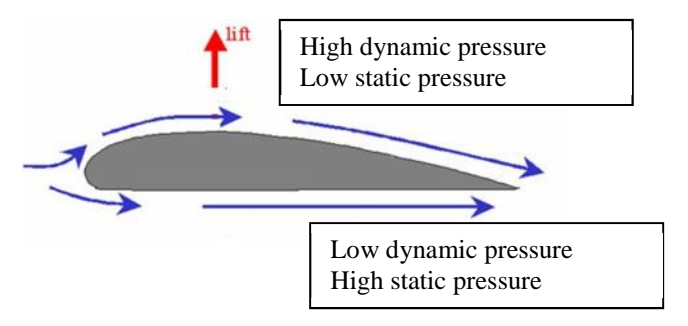


Figure 2: Lift generation on wing [2]

There are general methods that aim to accelerate the air stream over the upper surface of the wing such as increasing the angle of attack or increasing camber of wing as shown in Fig. 3.

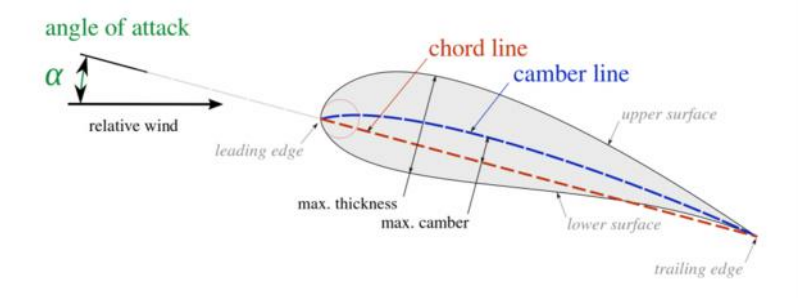


Figure 3: A schematic of typical airfoil [3]

For the propulsive wing, an embedded radial fan at the leading edge of wing (with its axis parallel to the leading edge) permits blowing of the air towards the trailing edge. Lift is generated from two sources; the circulation at the fan which pulls the air stream from leading edge toward the trailing edge of the wing with airflow adjacent to the upper surface of the wing which increases dynamic pressure and decreases static pressure on the upper surface of the wing. There is no influence from fan circulation on the bottom surface of the wing. The second source of lift is the vertical component of the reaction force on the wing resulting from the inclined velocity vector of the exiting airstream flow at the trailing edge. The horizontal component of the reaction force on the wing represents the thrust force, this results in a direct proportional relation between the speed of rotation of the fan (or throttle setting) and the lift acting on the wing, which is a feature rarely found in fixed wing aircraft as shown in Fig.4.

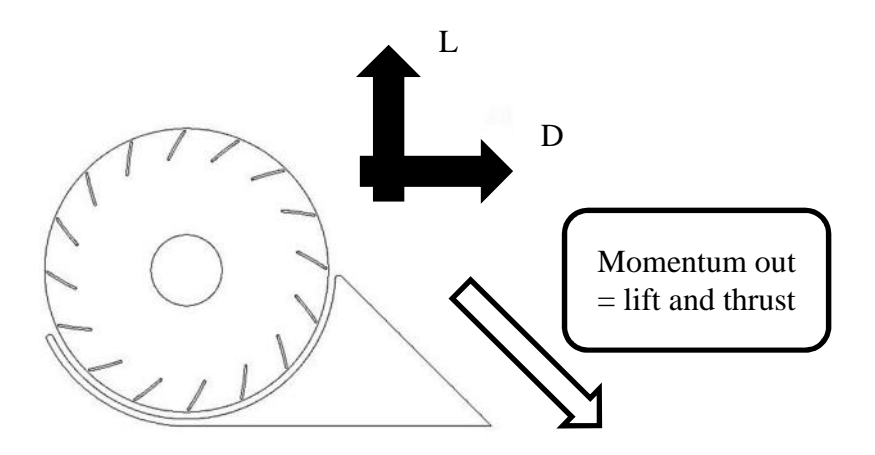


Figure 4: Schematic of propulsive wing cross section [4]

The concept of the propulsion wing is classified as one of the techniques of the embedded distributed systems. A full investigation by (Kim, 2010) [5] shows:

- Jet flaps (blowing engine exhaust out of the wing trailing edge).
- Cross-flow fan (two dimensional propulsor integrated within the wing trailing edge).

- Multiple discrete gas turbine engines (driven by their own power source).
- Distributed multi-fans driven by a limited number of gas turbine engine cores; which can be driven by conventional or electrical motors.

An investigation to study the advantages of distributed propulsion for future aircraft concepts was evaluated for six different integration approaches in order to down-select the best configuration as shown in Table 1 (Steiner, 2012) [6]. Categories included the integration of power system, the aspects of operation, weight, noise and efficiency. The evaluation is based on the boundary layer ingestion, which has the ability to increase aircraft efficiency by increasing the propulsive efficiency of the fans and shifting the optimum fan pressure ratio to higher values, hence permitting the use of a smaller propulsor size, which results in lower weight and drag of the propulsion system. The results show that the CROSS configuration is the best case and gives the highest efficiency for all embedded distributed systems.

Table 1: Distributed propulsion concepts [6]

Concept	Description and Abbreviation	
	Aft-mounted fans covering the upper part of a cylindrical fuselage (REVOLVE)	
	Blended Wing Bodies (BWB) with embedded fans on top of the lifting body trailing edge (BWB)	
A	Tube and wing configuration with fans integrated within a split-wing (SPLIT)	
	Tube and wing concept with fans mounted on the upper wing side (WING)	
	Cylindrical fuselage with circumferential fan at the aft section (PROPFUS)	
	Cross-flow fan embedded into the trailing edge of the wing (CROSS)	

An analysis of propulsive wing configurations according to the potentials of cross-flow fan for the application to commercial aircraft featuring extreme short takeoff and landing capabilities has been done by evaluating the kinematic mechanisms for three cross-flow fan propulsive airfoil concept solutions with a preliminary assessment enabling a low-speed operation as well as high-speed operation mode as shown in Fig.5. By using a thin supercritical airfoil in performing a two-dimensional simulation for concept (2) at a free stream velocity of 35 m/s for 15° angle of attack and a 12,000 RPM fan rotational speed, representing a potential take-off condition, the lift coefficient